MATCH
Communications in Mathematical and in Computer Chemistry

MATCH Commun. Math. Comput. Chem. **94** (2025) 135–155
ISSN: 0340–6253
doi: 10.46793/match.94-1.135D

Topological Isomers of DNA Dodecahedral Links

Jin-Wei Duan[a,*], **Xiao-Sheng Cheng**[b], **Tao Deng**[c]

[a]*School of Sciences, Chang'an University, Xi'an, Shaanxi, 710064, China.*

[b]*School of Mathematics and Statistics, Huizhou University, Huizhou, Guangdong, 516007, China.*

[c]*School of Mathematics and Computer Science, Northwest Minzu University, Lanzhou 730030, China.*

duanjw@chd.edu.cn

(Received December 23, 2024)

Abstract

A comprehensive understanding of the interrelationships among various DNA dodecahedral topological configurations holds immense theoretical significance for guiding experimental synthesis and practical applications. In this study, we investigate the topological isomers of DNA dodecahedral links. We defined DNA dodecahedral links with a consistent component number and genus as topological isomers. Two distinct strategies were employed to identify potential topological isomers. The HOMFLY-polynomial has been validated as a potent tool for distinguishing the topological isomers of DNA dodecahedral links. Our research not only provides valuable insights into the comprehensive understanding of DNA nanostructures but also offers clues for scientists to screen and synthesize unexplored DNA nanostructures.

*Corresponding author.

1 Introduction

Since DNA is conventionally recognized as an information storage material, it is also a versatile building material for the construction of various polyhedral configurations [1–3]. Scientists have successfully synthesized a variety of DNA nanostructures, which have demonstrated immense potential for drug delivery [4–6], disease diagnosis [7, 8], bioimaging technologies [9] and treatment due to their exceptional biocompatibility, programmability, addressability, and precisely controllable [10–13].

The dodecahedron, a unique geometric structure, offers a volume-to-surface-area ratio of a dodecahedral cage that is greater than that of its crystallographic counterparts, has been utilized in nanotechnology for the development of novel materials with different physical and chemical properties, particularly folding DNA / RNA strands in dodecahedral configurations [14, 15]. As an innovative nanomaterial and technology platform, DNA dodecahedra exhibits wide potential applications in the fields of nanoscale packaging materials, biomedical science, material science, and foundmental scientific research [16–19]. For example, DNA dodecahedra have been utilized to encapsulate and protect various biological or drug molecules [20], while also serving as nanoreactors for certain chemical reactions or biological processes [21].

The complexity and cost associated with the synthesis and assembly, ensuring stability and biocompatibility within living organisms, remain urgent. These challenges have prompted scientists to explore theoretical aspects more deeply to investigate diverse possibilities for DNA dodecahedral configurations. To provide a comprehensive overview of the number and diversity of dodecahedral DNA structures, topological methods have been introduced to systematically determine possible candidate structures that can be synthesized in laboratories [22, 23]. DNA polyhedral links, a topological model that represents DNA strands as dimensionless lines, have been proposed to describe and simulate artificial DNA structures [24–27]. A series of polyhedral links were constructed, and various topological indices were calculated, including component number (μ), crossing number (c), HOMFLY polynomial [28,29], braid index [30], etc. These indices have

contributed significantly to the design of novel polyhedral structures from a topological perspective. Consequently, the results suggest that DNA polyhedral links have great potential as templates for controlling chemical synthesis and have been validated [31].

It is worth noting that most previous studies have primarily focused on obtaining diverse configurations of DNA polyhedral links and exploring topological indexes. However, more attention should be paid to investigating the connections and distinctions among these various DNA polyhedral configurations, particularly those with identical topological indexes. We previously demonstrated potential relationships between various topological parameters associated with DNA polyhedral links. Our findings revealed that the genus g of a branched DNA polyhedral link depends not only on the number of components μ but also exhibits periodic variations [32]. This work lays the foundation for further exploration into the relationships among DNA dodecahedral configurations.

It is particularly intriguing to know whether there is a unique DNA dodecahedral configuration that can satisfy the given set of (μ, g). If not, it is plausible that one can have multiple different DNA dodecahedral configurations with the same genus and component number. These special configurations may exhibit diverse or even diametrically opposite properties, thereby affecting their practical applications. However, the precise definition and identification of these configurations remain an urgent issue, while the means to discern their distinctions have not yet been determined.

Therefore, it is necessary to define and distinguish these DNA dodecahedral configurations accurately. In this study, we defined DNA dodecahedral configurations with the same genus g and component number μ as topological isomers. These topological isomers were obtained by integrating the two strategies proposed by N. Jonoska [33, 34] and J. Duan [35], respectively. Subsequently, we employed the HOMFLY polynomials to discern the distinct characteristics of these topological isomers.

It is crucial to investigate their construction and analysis to facilitate the design and synthesis of DNA dodecahedra, providing theoretical guidelines for their rational design from a theoretical perspective. The study of topological isomers of DNA dodecahedral links not only enhances our

understanding of the relationship between topological indices of DNA polyhedral links but also offers valuable insights and potential candidates for experimental synthesis and application.

2 Methods

2.1 Define the topological isomers

A polyhedral link L is an interlinked and interlocked architecture obtained from a polyhedral graph G, utilizing tangle structures to replace its vertices and edges. To determine the genus of DNA polyhedral links, we introduce the Seifert algorithm [36], which provides an explicit method to find an orientable surface with one boundary component. As depicted in Figure 1a, each edge with $2k$ (or $2k$+1) half-turns will be transform to $2k$-1 (or $2k$) Seifert circles, while each vertex corresponds to a Seifert circle. The total Seifert number s is then calculated as the sum of the number of edge and vertex Seifert circles. For example, a given tetrahedral link is transformed into a configuration composed of several Seifert circles, as shown in Figure 1b. In this case, the total Seifert number is ten, comprising four vertex Seifert circles (blue, red, orange, and green) and six edge Seifert circles (purple).

Understanding the interrelationships between these topological indices, as each index corresponds to a specific configuration parameter,it is crucial to accurately providing a broader range of potential synthesis candidates. Hu was the first to reveal the relationship between component number (μ), crossing number (c), and Seifert number (s) based on the Seifert algorithm [37]. His results show that these three numbers satisfy a simple and elegant mathematical formula (1), called the new Euler formula for DNA polyhedra.

$$s + \mu - c = 2 - 2g \tag{1}$$

The formula serves as a crucial link connecting the topological parameters of DNA cages and the Euler characteristic of the corresponding polyhedron, facilitating the design of novel DNA polyhedra with a genus larger than 0. Li and his colleagues have extended this new formula to

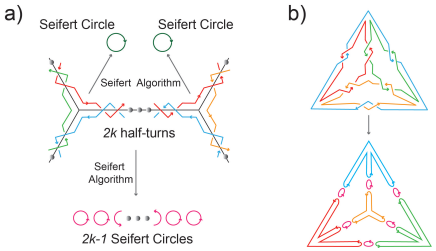

Figure 1. Schematic of Seifert algorithm on DNA polyhedral links. a)apply Seifert algorithm on vertexes and edges ; b) Schematic of Seifert algorithm on DNA tetrahedral links.

crossed DNA polyhedral links [38]. Duan and Hu have proposed a series of innovative design strategies to embed DNA polyhedral links into high-genus surfaces. These studies collectively demonstrate potential relationships between various topological parameters associated with DNA polyhedral links. In fact, the genus of a branched DNA polyhedral link depends not only on the number of components but also exhibits periodic variations [39], such as formula (2).

$$g = \frac{F - \mu}{2} \tag{2}$$

The component number μ reflects the required number of strands to construct a desired DNA polyhedron, while the genus represents an intrinsic property of the DNA polyhedral links. Using formula (2), we can observe that the genus varies with the component number of a given DNA polyhedral link. Therefore, revealing their relationship can provide valuable insight that guide synthesis strategies. Furthermore, it is imperative to address the challenge of distinguishing between different configurations of DNA polyhedral links that may have identical component numbers and genus. In this study, by incorporating the concept of allotropy in chemistry, we define DNA dodecahedral configurations with identical component number μ and genus g as topological isomers, denoted as (μ, g). Theoretically, formula (2) implies the potential existence of topological isomers of DNA dodecahedral links.

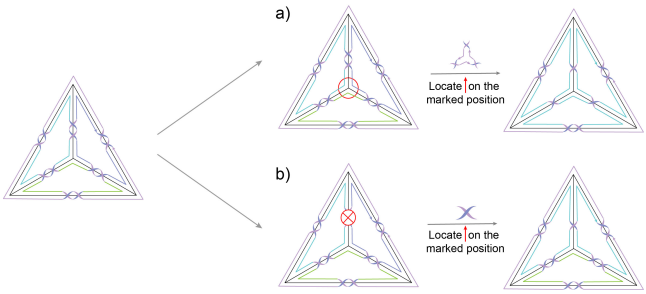

Figure 2. Construction of DNA tetrahedral links employing two diverse strategies.

2.2 Determin the topological isomers

However, the challenge to validate the existence of topological isomers remains. In this study, two strategies are employed to identify the potential topological isomers of DNA dodecahedral isomers. To illustrate the strategies, a DNA tetrahedral link with four components is chosen as the starting point,each edge being covered by even half-turns.

Strategy I: Duan and his colleague proposed an approach to replace vertex configurations with the minimum number of pseudo-surrounded vertices [35] (as shown in Figure 2a), thereby obtaining DNA polyhedral links with different numbers of components. For example, the central vertex (marked with a red circle) of the given tetrahedral link illustrated in Figure 2a can be designated as a pseudo-surrounded vertex, resulting in the tetrahedral link with two component numbers depicted in Figure 2a.

Strategy II: This strategy was proposed by N. Jonoska and R. Twarock [33, 34] , presenting a blueprint for organizing nucleic acid within a dodecahedral cage in such a way that the resulting product has minimal component number through adjusting even half-turns on selected edges of a DNA polyhedral configuration to odd half-turns. The even half-turns circled by a red circle (with crosses) are replaced by odd half-turns, as depicted in Figure 2b, resulting in a reduction of the number of components of the tetrahedral link from four to three (Figure 2b). Therefore, various DNA polyhedral configurations with different component numbers can be obtained based on this method.

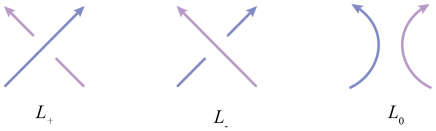

Figure 3. Crossing and smoothing changes on a local region of a link diagram

Therefore, both strategies are utilized in conjunction to assist us in identifying distinct topological isomers of the DNA icosahedral link that meet our requirements, ensuring an adequate number of configurations for analysis and comparison.Since the antiparallel property of the DNA double helix determines that the DNA polyhedral links must be antiparallel, verification is required. Therefore, for a dodecahedron, if there is an even number of odd half-turn edges on each face, then the corresponding DNA dodecahedron link must be antiparallel.

2.3 Distinct the topological isomers

When we successfully obtained the topological isomers, distingushing them became a critical challenge. Although mathematical methods exist to differentiate similar structures, such as employing types of polynomial, we opted to utilize the HOMFLY polynomial in this paper. The HOMFLY polynomial is a powerful invariant for knots and links, remaining unchanged under transformations, which allows for adequate distinction between different knots. It surpasses other invariants, like the Alexander and Jones polynomials, in its ability to differentiate complex knot types. Additionally, in certain cases, specific isomers can be represented as knots, enabling the potential use of the HOMFLY polynomial to distinguish them. Previous studies demonstrated that the HOMFLY polynomial is limited to isomers with apparent topological features, such as DNA polyhedral links. These attempts demonstrate the applicability of the HOMFLY polynomial in differentiating isomorphic variants, thereby providing valuable insight for our subsequent differentiation of topological isomers of DNA polyhedral links.

In this study, the framed version was introduced to the fore, for a link

L, we denote the evaluation of its HOMFLY polynomial by $P(L)$, which is defined by the following skein relations:

(1) $P(\text{unknot}) = 1$

(2) $\frac{1}{v}P_{L+} - vP_{L-} = zP_{L-}$

Where $L_+, L_-,$ and L_0 are the links formed by crossing and smoothing changes in a local region of a link diagram, as indicated in Figure 3. Then, the Kodama's program KnotGTK (http://www.math.kobe-u.ac.jp/∼ kodama/knot.html) was employed to calculate the HOMFLY polynomials of all topological isomers [40].

3 Results

3.1 DNA dodecahedra with six components

According to Strategy I, three vertices on the given dodecahedron were chosen and replaced by pseudo-surrounded vertices (Figure 4a, left), resulting in DNA dodecahedral configuration I with a component number of six (Figure 4a, right). Although there may be other ways to determine the positions of these three vertices, previous literature has shown that they are equivalent and confirmed that they have the same configuration [35].

Configuration II is obtained through Strategy II, with component number of six. Initially, 24 edges were circled, as depicted in Figure 4b (left), indicating the replacement of these even half-turn edges with odd half-turn edges. Subsequently, the final structure is presented in a simplified wireframe representation (Figure 4b, right). As well as configuration II, strategy II was also employed to obtain configuration III, which also consists of six components.

The Seifert number and the crossing number were calculated for configurations I, II and III, while formulas (1) and (2) were employed to determine the genus of these configurations. All three configurations were observed to exhibit a genus of three. Given their identical component number and genus, these configurations satisfy our definition of topological isomers, which are denoted as (6, 3) topological isomers of the DNA dodecahedral links.

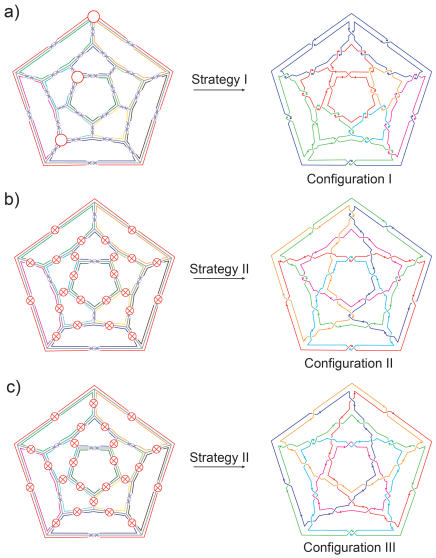

Figure 4. Construction of DNA dodecahedral links employing two diverse strategies. a) configuration I with six components; b) configuration II with six components; c) configuration III with six components.

Table 1. Details of (6, 3) dodecahedral topological isomers

Configuration	s	μ	c	F	g
I	41	6	51	12	3
II	26	6	36	12	3
III	26	6	36	12	3

To differentiate between these configurations, we utilized Kodama's KnotGTK program to compute the HOMFLY polynomials for each configuration. The results are presented in the following:

HOMFLY-polynomial of configuration I:

$P_I(v,z) = z^{-5}(v^{59}-11v^{57}+52v^{55}-138v^{53}+225v^{51}-231v^{49}+146v^{47}-52v^{45}+8v^{43}) + z^{-3}(-24v^{57}+228v^{55}-903v^{53}+1,923v^{51}-2,355v^{49}+1,620v^{47}-537v^{45}+39v^{43}+3v^{41}+6v^{39})+z^{-1}(259v^{55}-2,056v^{53}+6,462v^{51}-10,031v^{49}+7,565v^{47}-1,899v^{45}-418v^{43}+v^{41}+96v^{39}+17v^{37}+4v^{35})+z(-1,650v^{53}+10,372v^{51}-23,284v^{49}+20,346v^{47}-1,871v^{45}-4,288v^{43}-819v^{41}+700v^{39}+359v^{37}+126v^{35}+9v^{33})+z^3(6,823v^{51}-30,721v^{49}+37,127v^{47}+3,886v^{45}-17,558v^{43}-7,583v^{41}+2,592v^{39}+3,324v^{37}+1,650v^{35}+406v^{33}+51v^{31}+3v^{29})+z^5(-18,792v^{49}+47,885v^{47}+7,053v^{45}-45,301v^{43}-29,100v^{41}+6,048v^{39}+17,342v^{37}+12,342v^{35}+5,229v^{33}+1,582v^{31}+386v^{29}+75v^{27}+11v^{25}+v^{23})+z^7(33,414v^{47}-13,975v^{45}-77,636v^{43}-51,910v^{41}+20,635v^{39}+59,784v^{37}+54,630v^{35}+32,672v^{33}+15,034v^{31}+5,766v^{29}+1,875v^{27}+495v^{25}+93v^{23}+9v^{21})+z^9(-34,050v^{45}-62,089v^{43}-16,897v^{41}+75,088v^{39}+137,189v^{37}+138,983v^{35}+102,889v^{33}+61,527v^{31}+31,293v^{29}+13,822v^{27}+5,283v^{25}+1,704v^{23}+442v^{21}+84v^{19}+9v^{17})+z^{11}(14,019v^{43}+56,691v^{41}+114,444v^{39}+154,959v^{37}+159,420v^{35}+133,620v^{33}+95,395v^{31}+59,678v^{29}+33,231v^{27}+16,563v^{25}+7,371v^{23}+2,901v^{21}+992v^{19}+286v^{17}+66v^{15}+11v^{13}+v^{11})$

HOMFLY-polynomial of configuration II:

$P_{II}(v,z) = z^{-5}(-v^{17}+5v^{15}-10v^{13}+10v^{11}-5v^9+v^7)+z^{-3}(-7v^{17}+39v^{15}-84v^{13}+86v^{11}-39v^9+3v^7+2v^5)+z^{-1}(-10v^{17}+109v^{15}-314v^{13}+364v^{11}-152v^9-13v^7+12v^5+4v^3)+z(-3v^{17}+125v^{15}-626v^{13}+927v^{11}-342v^9-154v^7+29v^5+42v^3+2v)+z^3(108v^{15}-825v^{13}+1,600v^{11}-379v^9-684v^7-65v^5+214v^3+29v+2v^{-1})+z^5(-2v^{17}+81v^{15}-837v^{13}+1,988v^{11}-16v^9-1,766v^7-733v^5+540v^3+149v+19v^{-1}+v^{-3})+z^7(34v^{15}-605v^{13}+1,858v^{11}+657v^9-2,958v^7-2,288v^5+697v^3+388v+84v^{-1}+5v^{-3})+z^9(-v^{17}+19v^{15}-349v^{13}+1,332v^{11}+1,169v^9-3,570v^7-4,172v^5+163v^3+600v+207v^{-1}+18v^{-3})+z^{11}(-2v^{17}+30v^{15}-215v^{13}+770v^{11}+1,227v^9-3,238v^7-5,187v^5-933v^3+544v+304v^{-1}+38v^{-3})+z^{13}(-v^{17}+25v^{15}-158v^{13}+370v^{11}+963v^9-2,317v^7-4,696v^5-1,701v^3+215v+275v^{-1}+47v^{-3})+z^{15}(8v^{15}-94v^{13}+212v^{11}+571v^9-1,411v^7-3,097v^5-1,524v^3-$

$87v+133v^{-1}+30v^{-3})+z^{17}(-24v^{13}+119v^{11}+167v^9-728v^7-1,411v^5-800v^3-143v+23v^{-1}+9v^{-3})+z^{19}(28v^{11}-11v^9-250v^7-387v^5-230v^3-59v-3v^{-1}+v^{-3})+z^{21}(-11v^9-37v^7-46v^5-27v^3-8v-v^{-1})$

HOMFLY-polynomial of configuration III:

$P_{III}(v,z)=z^{-4}(2v^{20}-9v^{18}+16v^{16}-14v^{14}+6v^{12}-v^{10})+z^{-2}(5v^{20}-34v^{18}+77v^{16}-79v^{14}+42v^{12}-17v^{10}+8v^8-2v^6)+(v^{20}-52v^{18}+191v^{16}-258v^{14}+192v^{12}-149v^{10}+104v^8-29v^6)+z^2(2v^{20}-64v^{18}+387v^{16}-672v^{14}+555v^{12}-533v^{10}+469v^8-131v^6-11v^4-2v^2)+z^4(3v^{20}-87v^{18}+589v^{16}-1,234v^{14}+889v^{12}-1,034v^{10}+1,323v^8-303v^6-122v^4-24v^2)+z^6(v^{20}-42v^{18}+522v^{16}-1,345v^{14}+614v^{12}-1,182v^{10}+2,828v^8-124v^6-409v^4-149v^2-10)+z^8(-17v^{18}+252v^{16}-855v^{14}-271v^{12}-823v^{10}+4,545v^8+1,094v^6-615v^4-434v^2-60)+z^{10}(v^{20}-10v^{18}+121v^{16}-355v^{14}-831v^{12}-408v^{10}+5,499v^8+3,196v^6-230v^4-722v^2-168-5v^{-2})+z^{12}(v^{20}-13v^{18}+42v^{16}-63v^{14}-774v^{12}-311v^{10}+5,095v^8+4,622v^6+694v^4-638v^2-243-20v^{-2})+z^{14}(-8v^{18}+43v^{16}+54v^{14}-595v^{12}-166v^{10}+3,675v^8+4,056v^6+1,198v^4-227v^2-168-21v^{-2})+z^{16}(22v^{16}-27v^{14}-335v^{12}+135v^{10}+1,960v^8+2,208v^6+882v^4+58v^2-44-8v^{-2})+z^{18}(-24v^{14}-52v^{12}+187v^{10}+658v^8+680v^6+312v^4+59v^2-v^{-2})+z^{20}(9v^{12}+48v^{10}+94v^8+86v^6+41v^4+10v^2+1)$

The analysis of the HOMFLY polynomials reveals that despite having identical genus and component numbers, these (6, 3) dodecahedral topological isomers exhibit distinct topological properties. This highlights the effectiveness of the HOMFLY polynomial as a powerful tool for discerning their dissimilarities.

3.2 DNA dodecahedra with four components

The acquisition of configuration IV with four components by strategy I requires the presence of four pseudo-surrounded vertices, as depicted in Figure 5a. The positional distribution scheme of the four pseudo-surrounded vertices shown in Figure 5a (left) is unique, which is particularly noteworthy due to the equivalence of the 20 vertices of a dodecahedron. The final simplified wireframe configuration is presented in Figure 5a (right).

According to strategy II, a total of 24 odd half-turns are strategically positioned at distinct locations to substitute the corresponding even half-

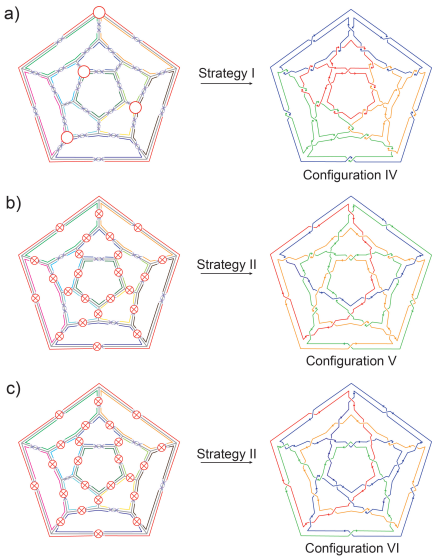

Figure 5. Construction of DNA dodecahedral links employing two diverse strategies. a) configuration VI with four components; b) configuration V with four components; c) configuration VI with four components.

turns, thereby effectively reducing the component count to four. The specific details can be observed in Figures 5b (left) and 5c (left), leading to the derivation of two distinct configurations denoted V and VI.

Subsequently, the Seifert algorithm was executed on the three configurations to determine their Seifert number s and the crossing number c. These values are listed in Table 2 and were then utilized in formulas (1) and (2) to calculate their genus g. Remarkably, it was observed that each configuration exhibited a genus of 4. Evidently, these three configurations can be classified as topological isomers based on the definition and should be designated as the (4, 4) dodecahedral topological isomers.

The KnotGTK program is employed to compute HOMFLY polynomials in configurations VI, V and VI. The findings suggest that the HOMFLY polynomials of the three (4, 4) dodecahedral topological isomers exhibit distinct variations, indicating their topological dissimilarity. The obtained HOMFLY polynomials are presented as follows:

HOMFLY-polynomial of configuration IV:

$P_{IV}(v,z) = z^{-3}(-v^{55}+11v^{53}-51v^{51}+129v^{49}-192v^{47}+168v^{45}-80v^{43}+16v^{41})+z^{-1}(22v^{53}-204v^{51}+762v^{49}-1,446v^{47}+1,422v^{45}-618v^{43}+38v^{41}+24v^{37})+z(-215v^{51}+1,607v^{49}-4,420v^{47}+5,098v^{45}-1,488v^{43}-954v^{41}-43v^{39}+301v^{37}+79v^{35}+35v^{33})+z^3(1,220v^{49}-6,758v^{47}+10,822v^{45}-1,052v^{43}-6,423v^{41}-1,787v^{39}+1,893v^{37}+1,511v^{35}+775v^{33}+213v^{31}+18v^{29})+z^5(-4,383v^{47}+14,777v^{45}-1,197v^{43}-19,773v^{41}-9,839v^{39}+7,131v^{37}+11,172v^{35}+7,662v^{33}+3,259v^{31}+899v^{29}+192v^{27}+32v^{25}+4v^{23})+z^7(10,002v^{45}-8,714v^{43}-34,312v^{41}-18,236v^{39}+22,058v^{37}+42,826v^{35}+37,183v^{33}+21,313v^{31}+9,016v^{29}+3,068v^{27}+852v^{25}+174v^{23}+18v^{21})+z^9(-13,119v^{43}-24,761v^{41}+193v^{39}+53,581v^{37}+90,979v^{35}+90,217v^{33}+64,359v^{31}+36,039v^{29}+16,711v^{27}+6,555v^{25}+2,148v^{23}+562v^{21}+108v^{19}+12v^{17})+z^{11}(6,474v^{41}+28,710v^{39}+61,881v^{37}+87,039v^{35}+90,576v^{33}+74,864v^{31}+51,521v^{29}+30,483v^{27}+15,786v^{25}+7,194v^{23}+2,871v^{21}+989v^{19}+286v^{17}+66v^{15}+11v^{13}+v^{11})$

HOMFLY-polynomial of configuration V:

$P_V(v,z) = z^{-3}(-v^{37}+3v^{35}-3v^{33}+v^{31})+z^{-1}(v^{39}-12v^{37}+35v^{35}-38v^{33}+26v^{31}-24v^{29}+12v^{27})+z(-2v^{39}-29v^{37}+148v^{35}-113v^{33}-22v^{31}-137v^{29}+137v^{27}+17v^{25}+v^{23})+z^3(-v^{39}-6v^{37}+368v^{35}-340v^{33}-783v^{31}-185v^{29}+860v^{27}+298v^{25}+29v^{23})+z^5(35v^{37}+375v^{35}-1,157v^{33}-2,532v^{31}+584v^{29}+3,671v^{27}+2,077v^{25}+461v^{23}+38v^{21})+z^7(10v^{37}-38v^{35}-1,823v^{33}-2,858v^{31}+3,180v^{29}+9,141v^{27}+6,920v^{25}+2,637v^{23}+608v^{21}+90v^{19}+6v^{17})+z^9(-v^{37}-95v^{35}-824v^{33}-251v^{31}+5,658v^{29}+11,701v^{27}+10,625v^{25}+5,762v^{23}+2,163v^{21}+596v^{19}+114v^{17}+12v^{15})+z^{11}(v^{35}+87v^{33}+981v^{31}+3,494v^{29}+5,967v^{27}+6,028v^{25}+4,149v^{23}+2,137v^{21}+863v^{19}+274v^{17}+66v^{15}+11v^{13}+v^{11})$

HOMFLY-polynomial of configuration VI:

$P_{VI}(v,z) = z^{-3}(v^{39}-5v^{37}+9v^{35}-7v^{33}+2v^{31})+z^{-1}(3v^{39}-34v^{37}+82v^{35}-56v^{33}-13v^{31}+18v^{29})+z(-3v^{39}-53v^{37}+278v^{35}-193v^{33}-240v^{31}+139v^{29}+66v^{27}+6v^{25})+z^3(-v^{39}-4v^{37}+503v^{35}-570v^{33}-1,212v^{31}+527v^{29}+756v^{27}+208v^{25}+17v^{23})+z^5(36v^{37}+408v^{35}-1,445v^{33}-2,882v^{31}+1,587v^{29}+3,784v^{27}+1,907v^{25}+408v^{23}+36v^{21})+z^7(10v^{37}-38v^{35}-1,955v^{33}-2,904v^{31}+4,035v^{29}+9,534v^{27}+6,875v^{25}+2,577v^{23}+596v^{21}+90v^{19}+6v^{17})+z^9(-v^{37}-95v^{35}-840v^{33}-189v^{31}+6,040v^{29}+11,996v^{27}+10,706v^{25}+5,761v^{23}+2,154v^{21}+594v^{19}+114v^{17}+12v^{15})+z^{11}(v^{35}+$

Table 2. Details of (4, 4) dodecahedral topological isomers

Configuration	s	μ	c	F	g
IV	38	4	48	12	4
V	26	4	36	12	4
VI	26	4	36	12	4

Table 3. Details of (2, 5) dodecahedral topological isomers

Configuration	s	μ	c	F	g
VII	35	2	45	12	5
VIII	26	2	36	12	5

$87v^{33} + 996v^{31} + 3,556v^{29} + 6,033v^{27} + 6,065v^{25} + 4,162v^{23} + 2,139v^{21} + 863v^{19} + 274v^{17} + 66v^{15} + 11v^{13} + v^{11})$

3.3 DNA dodecahedra with two components

To obtain configuration VII with two components, as shown in Figure 6a based on strategy I, it is necessary to position five pseudo-surrounded vertices at different locations. It should be noted that Figure 6a only displays the result. In fact, a two-step approach is required to determine the locations instead of placing all five pseudo-surrounded vertices simultaneously. Firstly, four pseudo-surrounded vertices are needed to achieve configuration IV and reduce the number of components to four. Secondly, the fifth pseudo-surrounded vertex should be placed strategically to further decrease the component count to two. According to strategy II, a total of 24 odd half-turns are still employed to replace the precisely positioned even half-turns, resulting in the achievement of configuration VIII comprising two components (as shown in Figure 6b).

The Seifert number, crossing number and genus have been calculated and are presented in Table 3. In accordance with the definition, it is also imperative to consider both configurations as topological isomers, denoted by the term (2, 5) dodecahedral topological isomers.

The HOMFLY polynomials of two (2, 5) dodecahedral topological isomers were computed using the KnotGTK program. The obtained results suggest that the two configurations exhibit distinct topological character-

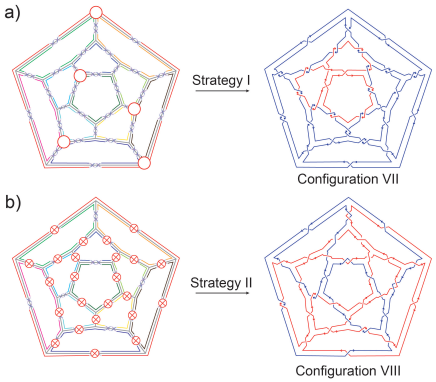

Figure 6. Construction of DNA dodecahedral links employing two diverse strategies. a) configuration VII with 2 components; b) configuration VIII with 2 components.

istics. The specific HOMFLY polynomials are presented below:

HOMFLY-polynomial of configuration VII:

$P_{VII}(v,z) = z^{-1}(v^{51} - 11v^{49} + 43v^{47} - 69v^{45} + 20v^{43} + 60v^{41} - 43v^{39} - 19v^{37} + 18v^{35}) + z(-20v^{49} + 177v^{47} - 480v^{45} + 249v^{43} + 720v^{41} - 741v^{39} - 235v^{37} + 250v^{35} + 74v^{33} + 15v^{31}) + z^3(175v^{47} - 1,143v^{45} + 1,435v^{43} + 2,560v^{41} - 4,025v^{39} - 2,010v^{37} + 1,603v^{35} + 1,294v^{33} + 513v^{31} + 111v^{29} + 3v^{27}) + z^5(-867v^{45} + 3,403v^{43} + 2,866v^{41} - 11,707v^{39} - 7,614v^{37} + 5,985v^{35} + 8,882v^{33} + 5,405v^{31} + 2,017v^{29} + 462v^{27} + 75v^{25} + 6v^{23}) + z^7(2,592v^{43} - 2,105v^{41} - 18,754v^{39} - 10,985v^{37} + 17,129v^{35} + 30,926v^{33} + 25,135v^{31} + 13,421v^{29} + 5,216v^{27} + 1,586v^{25} + 370v^{23} + 56v^{21} + 3v^{19}) + z^9(-4,362v^{41} - 11,205v^{39} + 1,955v^{37} + 34,719v^{35} + 57,327v^{33} + 54,874v^{31} + 37,453v^{29} + 19,898v^{27} + 8,668v^{25} + 3,151v^{23} + 940v^{21} + 219v^{19} + 36v^{17} + 3v^{15}) + z^{11}(2,481v^{39} + 13,230v^{37} + 30,948v^{35} + 44,616v^{33} + 46,013v^{31} + 36,907v^{29} + 24,270v^{27} + 13,533v^{25} + 6,507v^{23} + 2,703v^{21} + 959v^{19} + 283v^{17} + 66v^{15} + 11v^{13} + v^{11})$

HOMFLY-polynomial of configuration VIII:

$P_{VIII}(v,z) = z^{-1}(v^{39} - 8v^{37} + 22v^{35} - 25v^{33} + 10v^{31}) + z(-3v^{39} - 12v^{37} + 130v^{35} - 173v^{33} - 65v^{31} + 111v^{29} + 24v^{27}) + z^3(-v^{39} + 16v^{37} + 322v^{35} - 603v^{33} - 818v^{31} + 684v^{29} + 674v^{27} + 141v^{25} + 9v^{23}) + z^5(36v^{37} + 309v^{35} - 1,504v^{33} - 2,447v^{31} + 2,119v^{29} + 3,900v^{27} + 1,754v^{25} + 361v^{23} + 36v^{21}) + z^7(10v^{37} - 56v^{35} - 1,999v^{33} - 2,600v^{31} + 4,674v^{29} + 9,914v^{27} + 6,818v^{25} +$

$2,513v^{23} + 586v^{21} + 90v^{19} + 6v^{17}) + z^9(-v^{37} - 95v^{35} - 845v^{33} - 47v^{31} + 6,380v^{29} + 12,302v^{27} + 10,792v^{25} + 5,755v^{23} + 2,142v^{21} + 591v^{19} + 114v^{17} + 12v^{15}) + z^{11}(v^{35} + 87v^{33} + 1,019v^{31} + 3,619v^{29} + 6,111v^{27} + 6,114v^{25} + 4,180v^{23} + 2,142v^{21} + 863v^{19} + 274v^{17} + 66v^{15} + 11v^{13} + v^{11})$

4 Discussion

The more complex the geometric structure, the greater the possibility of encountering topological isomers. Therefore, in this study, we defined DNA dodecahedral configurations having identical genus and component number as topological isomers. Subsequently, two strategies were utilized to determine the potential topological isomers of DNA dodecahedral links. The HOMFLY-polynomials of these topological isomers were calculated by KnotGTK to characterize their differences. Based on the results, it can be concluded that topological isomers of DNA dodecahedral links truly exist, and the HOMFLY polynomial has been demonstrated as a suitable tool for their discrimination.

In compariing the findings with previous studies [41–44], it must be pointed out that the majority of works focused on obtaining diverse configurations of DNA polyhedral links, but the connections and differences between these configurations have not been paid sufficient attention. This hinders the discovery of topological isomers and the deep understanding of DNA dodecahedral links. This study presents a theoretical definition of topological isomers and employs two alternative methods to construct topological isomers of DNA dodecahedral links. It is worth noting that the strategy I represents the most convenient approach for obtaining topological isomers, while the strategy II offers a more comprehensive search for isomers. Therefore, combining both strategies becomes essential to maximize the discovery of topological isomers of DNA dodecahedral links.

These topological configurations will hopefully serve as useful candidates for experimental synthesis and may play different roles in various application fields. For instance, isomers II, V and VIII all exhibit six edges with even half-turns; however, their distribution patterns differ. Obviously, the different distribution of the six edges will lead to varing

component numbers and genus, thus providing theoretical design details for these DNA dodecahedra. The spatial configurations of isomers II and III, which have the same number of components and genus, are different; therefore, the design details for their experimental synthesis are also different.

Despite its limitations, this study provides insights into the definition, construction, and differentiation of topological isomers of DNA dodecahedral links. However, several unanswered questions persist. Firstly, the manual determination of all topological isomers remains infeasible, further endeavors are needed to explore suitable methods for their identification. Secondly, the quest for a more efficient and straightforward approach to distinguish topological isomers continues. Additionally, the proposed strategy in this study necessitates additional verification, particularly regarding the applicability of polynomials in discerning topological isomers of other polyhedra.

Thus, the integration of our strategies in future endeavors may facilitate the development of customized algorithms, which could exhibit even greater efficacy in accurately determining all topological isomers of DNA dodecahedral links, even of DNA polyhedral links. To facilitate the design and synthesis of DNA dodecahedra, it is crucial to investigate their construction and analysis while providing theoretical guidelines for their rational design from a theoretical perspective. Our work not only enhances our understanding of the relationship between topological indices of DNA polyhedral links but also offers valuable insights and potential candidates for experimental synthesis.

***Acknowledgment*:** J. W. Duan is supporeted by the Natural Science Foundation of Shaanxi Province (Grant 2020JM-266); X. S. Cheng is supported by Huizhou City Basic Education educational science research project (No. 2023hzkt193) and Teachng Quality and Teaching Reform Project of Huizhou University (No. 158[2023]); and T. Deng is supported by the National Natural Science Foundation of China (Grant 32060234). The authors are very thankful to the anonymous reviewers for their useful comments and suggestions, which helped us refine and enhance this paper.

References

[1] N. Seeman, H. Sleiman, DNA nanotechnology, *Nat. Rev. Mat.* **3** (2018) #17068.

[2] S. Kosara, R. Singh, D. Bhatia, Structural DNA nanotechnology at the nexus of next-generation bio-applications: challenges and perspectives, *Nanoscale Adv.* **6** (2024) 386–401.

[3] N. Seeman, Nanomaterials based on DNA, *Annu. Rev. Biochem.* **79** (2010) 65–87.

[4] T. Wang, Y. Liu, Q. Wu, B. Lou, Z. Liu, DNA nanostructures for stimuli-responsive drug delivery, *Smart Mat. Medicine* **3** (2022) 66–84.

[5] Q. Hu, H. Li, L. Wang, H. Gu, C. Fan, DNA nanotechnology-enabled drug delivery systems, *Chem. Rev.* **119** (2019) 6459–6506.

[6] M. Kumar, A. Jha, B. Mishra, DNA-based nanostructured platforms as drug delivery systems, *Chem. Bio. Eng.* **1** (2024) 179–198.

[7] W. Ma, Y. Zhan, Y. Zhang, C. Mao, X. Xie, Y. Lin, The biological applications of DNA nanomaterials: current challenges and future directions, *Sig. Transduct. Target Ther.* **6** (2021) #351.

[8] T. Chen, L. Ren, X. Liu, M. Zhou, L. Li, J. Xu, X. Zhu, DNA nanotechnology for cancer diagnosis and therapy, *Int. J. Mol. Sci.* **19** (2018) #1671.

[9] Q. Yang, X. Chang, J. Y. Lee, T. R. Olivera, M. Saji, H. Wisniewski, S. Kim, F. Zhang, Recent advances in self-assembled DNA nanostructures for bioimaging, *ACS Appl. Bio. Mat.* **5** (2022) 4652–4667.

[10] J. Liu, L. Song, S. Liu, Q. Jiang, Q. Liu, N. Li, Z. Wang, B. Ding, A DNA-based nanocarrier for efficient gene delivery and combined cancer therapy, *Nano Lett.* **18** (2018) 3328–3334.

[11] Q. Mou, Y. Ma, G. Pan, B. Xue, D. Yan, C. Zhang, X. Zhu, DNA trojan horses: self-assembled floxuridine-containing DNA polyhedra for cancer therapy, *Angew. Chem. Int. Ed.* **56** (2017) 12528–12532.

[12] A. Tay, N. Melosh, Nanostructured materials for intracellular cargo delivery, *Acc. Chem. Res.* **52** (2019) 2462–2471.

[13] S. Zhao, F. Duan, S. Liu, T. Wu, Y. Shang, R. Tian, J. Liu, Z. Wang, Q. Jiang, B. Ding, Efficient intracellular delivery of RNase A using DNA origami carriers, *ACS Appl. Mater. Interfaces* **11** (2019) 11112–11118.

[14] J. Zimmermann, M. Cebulla, S. Mönninghoff, G. von Kiedrowski, Self-assembly of a DNA dodecahedron from 20 trisoligonucleotides with C3h linkers, *Angew Chem. Int. Ed.* **47** (2008) 3626–3630.

[15] H. Li, K. Zhang, D. Binzel, L. Shlyakhtenko, Y. Lyubchenko, W. Chiu, P. Guo, RNA nanotechnology to build a dodecahedral genome of single-stranded RNA virus, *RNA Biol.* **18** (2021) 2390–2400.

[16] A. Chandrasekaran, O. Levchenko, DNA nanocages, *Chem. Mat.* **28** (2016) 5569–5581.

[17] L. Fang, C. Shi, Y. Wang, Z. Xiong, Y. Wang, Exploring the diverse biomedical applications of programmable and multifunctional DNA nanomaterials, *J. Nanobiotech.* **21** (2023) #290.

[18] G. Hu, Z. Wang, W. Qiu, A survey on mathematical models for DNA polyhedra, *MATCH Commun. Math. Comput. Chem.* **70** (2013) 725–742.

[19] X. Cheng, Q. Deng, Y. Diao, Constructions of DNA and polypeptide cages based on plane graphs and odd crossing π-junctions, *Appl. Math. Comput.* **43** (2023) #127773.

[20] D. Bhatia, S. Surana, S. Chakraborty, S. Koushika, Y. Krishnan, A synthetic icosahedral DNA-based host–cargo complex for functional in vivo imaging, *Nat. Commun.* **2** (2011) #339.

[21] X. Xu, J. Fu, X. Jiao, Y. Wang, C. Yao, DNA-induced assembly of biocatalytic nanocompartments for sensitive and selective aptasensing of aflatoxin B1, *Anal. Chim. Acta* **1295** (2024) #342328.

[22] W. Qiu, X. Zhai, Y. Qiu, The architecture of Platonic polyhedral links, *Sci. Chin. Ser. B Chem.* **51** (2008) 13–19.

[23] G. Hu, X. Zhai, D. Lu, W. Qiu, The architecture of Platonic polyhedral links, *J. Math. Chem.* **46** (2009) 592–603.

[24] W. Qiu, X. Zhai, Molecular design of Goldberg polyhedral links, *J. Mol. Struct. Theochem* **756** (2005) 163–166.

[25] K. Deng, J. Qian, F. Zhang, Enumerating DNA polyhedral links, *J. Math. Chem.* **51** (2013) 1329–1342.

[26] J. Duan, L. Cui, Y. Wang, H. Zheng, An approach to generate DNA polyhedral links of one/two strands, *J. Mol. Graph. Model.* **97** (2020) #107565.

[27] N. Wakayama, K. Shimokawa, On the classification of polyhedral links, *Symmetry* **14** (2022) #1712.

[28] M. Li, Q. Deng, X. Jin, A general method for computing the HOMFLY polynomial of DNA double crossover 3-regular links, *PLoS One* **10** (2015) #e0125184.

[29] S. Liu, X. Cheng, H. Zhang, W. Qiu, The architecture of polyhedral links and their HOMFLY polynomials, *J. Math. Chem.* **48** (2010) 439–456.

[30] X. Cheng, Y. Diao, The braid index of DNA double crossover polyhedral links, *PLoS One* **15** (2020) #e0228855.

[31] T. Sawada, A. Saito, K. Tamiya, K. Shimokawa, Y. Hisada, M. Fujita, Metal–peptide rings form highly entangled topologically inequivalent frameworks with the same ring- and crossing-numbers, *Nat. Commun.* **10** (2019) #921.

[32] J. Duan, G. Hu, W. Qiu, Topological aspect of DNA cages: genus, *MATCH Commun. Math. Comput. Chem.* **72** (2014) 475–488.

[33] N. Jonoska, R. Twarock, Blueprints for dodecahedral DNA cages, *J. Phys. Math. Theor.* **41** (2008) #304043.

[34] N. Grayson, A. Taormina, R. Twarock, DNA duplex cage structures with icosahedral symmetry, *Theor. Comput. Sci.* **410** (2009) 1440–1447.

[35] J. Duan, L. Cui, Y. Wang, Rational design of DNA Platonic polyhedra with the minimal components number from topological perspective, *Biochem. Biophys. Res. Commun.* **523** (2020) 627–631.

[36] H. Seifert, Uber das geschlecht von knoten, *Math. Ann.* **110** (1935) 570–592.

[37] G. Hu, W. Qiu, A. Ceulemans, A new Euler's formula for DNA polyhedra, *PLoS One* **6** (2011) #e26308.

[38] X. Li, W. Wang, W. Qiu, The new Euler's formula of the crossed DNA polyhedral links, *MATCH Commun. Math. Comput. Chem.* **70** (2013) 365–382.

[39] J. Duan, W. Li, X. Li, G. Hu, W. Qiu, Molecular design of DNA polyhedra based on genus, *J. Math. Chem.* **52** (2014) 2380–2394.

[40] K. Kodama, KnotGTK, `http://www.math.kobe-u.ac.jp/$\sim$kodama/knot.html`

[41] S. Liu, L. Guo, H. Bai, J. Hao, A topological approach to assembling strands–based DNA tetrahedra, *MATCH Commun. Math. Comput. Chem.* **81** (2019) 209–244.

[42] X. Jin, X. Cheng, Topological chirality of a type of DNA and protein polyhedral links, *J. Math. Chem.* **53** (2015) 1791–1807.

[43] T. Deng, Configuration of DNA polyhedra of truncated tetrahedron, cuboctahedron, truncated octahedron, *J. Theor. Biol.* **472** (2019) 4–10.

[44] J. Duan, L. Cui, Y. Wang, J. Zhang, Approaching the limit: molecular design of DNA prisms and pyramids with one strand based on polyhedral links, *MATCH Commun. Math. Comput. Chem.* **83** (2020) 345–356.